Supporting Information for:

In-situ Study of Ferroelectric-Antiferroelectric Phase Transition in $Hf_{1-x}Zr_xO_2$ at Elevated Temperatures up to 600 °C

Kisoo Nam[1,2,†], Zehao Lin[1,2,†], Tae Ryong Kim[1], Chang Niu[1,2], Sumi Lee[1,2], Shengyao Huang[1,2], Juanjuan Lu[3], Chang Liu[3], Sumeet K. Gupta[1], Haiyan Wang[1,3], and Peide D. Ye[1,2,]*

[1]Elmore Family School of Electrical and Computer Engineering, Purdue University, West Lafayette, IN 47907, United States

[2]Birck Nanotechnology Center, Purdue University, West Lafayette, IN 47907, United States

[3]School of Materials Engineering, Purdue University, West Lafayette, IN 47907, United States

†These authors contributed equally to this work: Kisoo Nam, Zehao Lin

* Correspondence and requests for materials should be addressed to P. D. Y. (yep@purdue.edu)

Supporting Note 1:

In some current density-electric field (J-E) hysteresis loops, three current density (J) peaks are observed in the first and second quadrants, while only two appear in the third and fourth quadrants. This asymmetry arises from the measurement method employed. **Figure S1** compares two different pulse schemes and their corresponding J-E hysteresis loops measured at 175 ˚C.

When a positive voltage is applied first, followed by a negative voltage, a total of five current density peaks are observed, as shown in red J-E hysteresis loop. This occurs because the coercive electric field (E_c) is slightly greater than 0%V, allowing additional polarization switching to occur during the application of the positive pulse in certain $Hf_{0.5}Zr_{0.5}O_2$ (HZO) grains. As a result, it appears that total three distinct switching events (E_c values) in first and second quadrant.

Conversely, when a negative voltage is applied first, followed by a positive voltage, the slightly positive E_c prevents polarization switching during the initial negative sweep to -1.4%V. Instead, switching occurs only at the end of the pulse, resulting in a total of four observable J peaks. Notably, the four J peaks observed in the blue J-E hysteresis loop align closely with four of the peaks in the red J-E loop, confirming that one of the five peaks in the red loop should be regarded as a "dummy" peak introduced by the pulse scheme. Therefore, only four intrinsic switching events occur within the system.

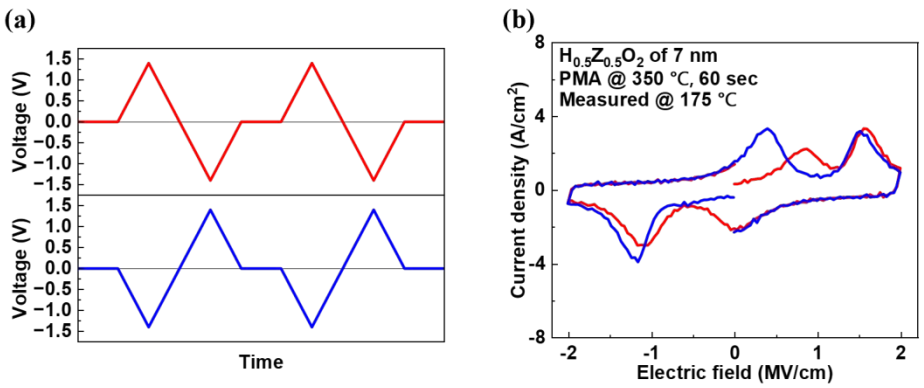

Figure S1. (a) Two different pulse schemes applied to 7 nm thick $Hf_{0.5}Zr_{0.5}O_2$ capacitors. (b) The corresponding J-E hysteresis loops measured at 175 ˚C. In the red curve, a total of five J peaks are observed, whereas in the blue curve, only four J peaks appear. The four peaks in the blue curve align closely with four of the peaks in the red curve, indicating that one of the five peaks in the red curve is a "dummy" peak introduced by the measurement method.

Supporting Note 2:

Figure S2(a) presents the evolution of the negative coercive electric field ($-E_c$). Only -Ec values are analyzed here because, as discussed in Supporting Note 1, the positive coercive field ($+E_c$) contains a dummy peak introduced by the measurement method, making accurate analysis unreliable. From the $-E_c$ trends, we clearly observe the point at which a single $-E_c$ value splits into two, indicating the onset of the ferroelectric (FE)-antiferroelectric (AFE) transition. Notably, this splitting point shifts depending on the thickness of the HZO film.

Figure S2(b) shows the $-E_c$ variation for samples subjected to different post-metal annealing (PMA) durations. These results demonstrate that shorter PMA durations lead to earlier $-E_c$ splitting, suggesting that the FE-AFE transition temperature is sensitive to annealing conditions. This behavior is likely because the orthorhombic (o) phase evolves from the tetragonal (t) phase through slight lattice symmetry breaking,[1-2] and shorter annealing promotes a lower fraction of the o phase. As a result, shorter PMA durations result in lower transition temperatures

Figure S2(c) summarizes the extracted transition temperatures as functions of both HZO thickness and PMA duration. The data confirm that thinner films and shorter annealing durations result in lower transition temperatures.

Additionally, the temperature-dependent polarization-electric field (P-E) and J-E hysteresis behavior of a 5%nm thick HZO film was investigated. As shown in **Figure S3(a)** and **(b)**, no FE response is observed at room temperature. This is attributed to the enhanced influence of the t

phase “dead layer” at the W/HZO interface.[3] The thinner the film, the more pronounced this interfacial effect becomes due to the higher surface energy. Consequently, the fraction of o phase become smaller than the fraction of t phase, which leads transition temperature become lower than room temperature. Substantial leakage current is observed at room temperature in the 5%nm-thick HZO sample, which increases further with temperature, complicating precise analysis. Nevertheless, a persistent plateau in the P-E loop is observed, indicating that AFE behavior remains even at elevated temperatures.

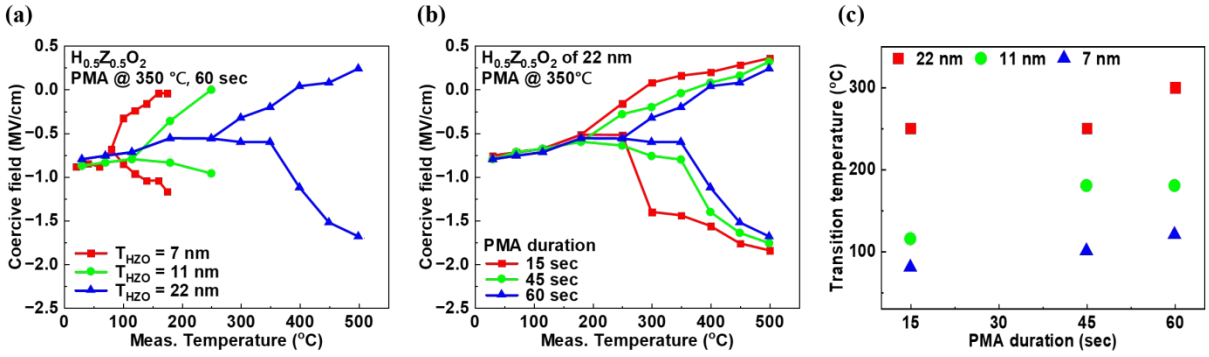

Figure S2. (a) Evolution of the -Ec with temperature for HZO capacitors of different thicknesses, showing that thinner films undergo the FE-AFE transition at lower temperatures. (b) Evolution of the -Ec with temperature for samples with different PMA durations. Shorter PMA durations result in an earlier onset of the FE-AFE transition. (c) Summary of the extracted transition temperatures as functions of HZO thickness and PMA duration.

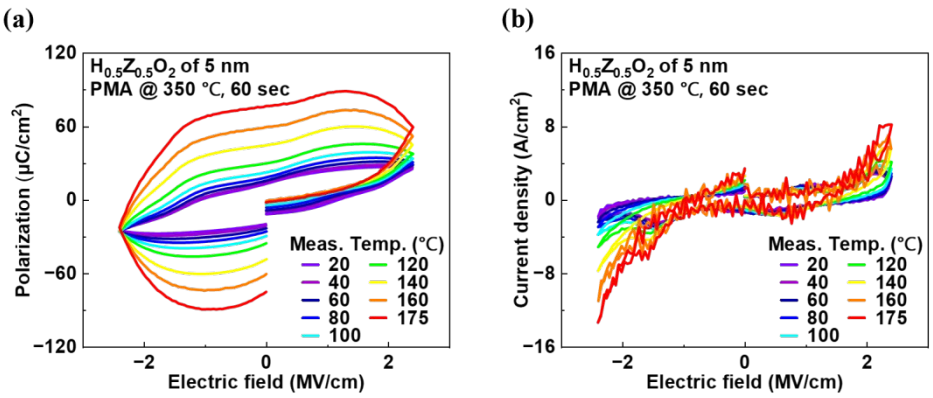

Figure S3. Temperature-dependent experimental data of 5 nm-thick $H_{0.5}Z_{0.5}O_2$ capacitors. The P-E and J-E hysteresis loops exhibit no observable FE behavior, and consequently, no FE-AFE transition is detected. (a-b) As the temperature increases, the effect of leakage current becomes more pronounced, leading to an apparent increase in polarization and current density value.

Supporting Note 3:

A sub-lattice phase-field simulation was performed to further support the phase transition mechanism proposed based on the Landau-Devonshire (L-D) analysis.[4] In this approach, the system is described by solving the time-dependent Ginzburg-Landau (TDGL) and Poisson equations, enabling the capture of domain evolution under varying thermal and electrical conditions. The model incorporates dipole-dipole (DD) and elastic interactions between neighboring sub-lattices, characterized by parameters h and g_x, respectively, as illustrated in **Figure S4(a)**.[5-6]

Figure S4(b) presents the simulated polarization distributions across individual sub-lattices under various temperature and electric field conditions. Starting from 300%˚C, the application of voltage clearly reveals the coexistence of o and t phases, consistent with experimental observations.

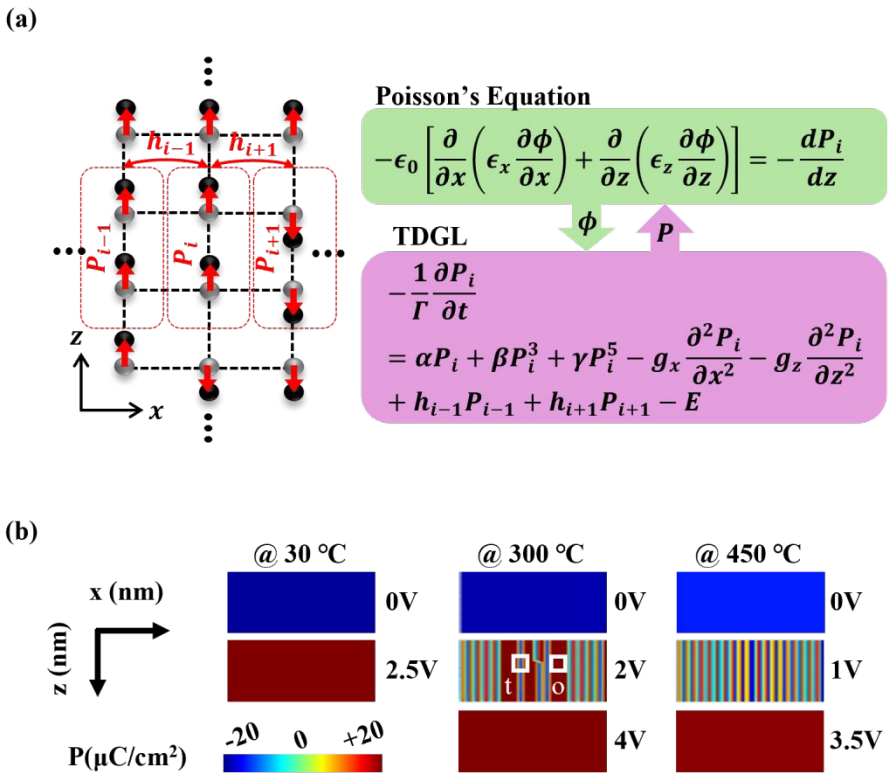

Figure S4. (a) Simulation process flow for an HZO capacitor. The sub-lattice phase-field model solves the time-dependent Ginzburg-Landau (TDGL) equation coupled with Possion's equation. Dipole-dipole and elastic interactions with adjacent sub-lattices are captured through h_{i-1}, h_{i+1}, and g_x. (b) Simulated polarization maps within a single grain under different temperature and bias conditions.

Supporting Note 4:

The temperature-dependent polarization behavior of $Hf_{1-x}Zr_xO_2$ capacitors with relatively thick films (>20%nm) and varying compositions was also investigated. As shown in **Figure S5(a)**, the 20%nm thick pure HfO_2 capacitor exhibited no observable FE or AFE response up to 600%˚C. Only above 550%˚C did the P-E hysteresis loop begin to widen, which can be attributed to increased leakage current.

In contrast, the 22%nm thick $Hf_{0.75}Zr_{0.25}O_2$ capacitor exhibited a clear FE response across the entire temperature range, although significant leakage current effects became noticeable above 550%˚C (**Figure S5(b)**).

Meanwhile, the 20%nm thick $Hf_{0.25}Zr_{0.75}O_2$ capacitor exhibited AFE behavior even at room temperature. As shown in **Figure S5(c)** and consistent with **Figure 4(c)** in the main text, both the maximum polarization (P_{max}) and remanent polarization (P_r) gradually decreased with increasing temperature.[7-9]

These results indicate that even in thicker films, the FE-AFE transition temperature is strongly composition-dependent. Specifically, the $Hf_{0.75}Zr_{0.25}O_2$ composition exhibits a very high transition temperature, whereas for $Hf_{0.25}Zr_{0.75}O_2$, the transition temperature is lower than room temperature.

Figure S6 summarizes the FE-AFE transition temperature across different film thicknesses and compositions in $Hf_{1-x}Zr_xO_2$ capacitors.

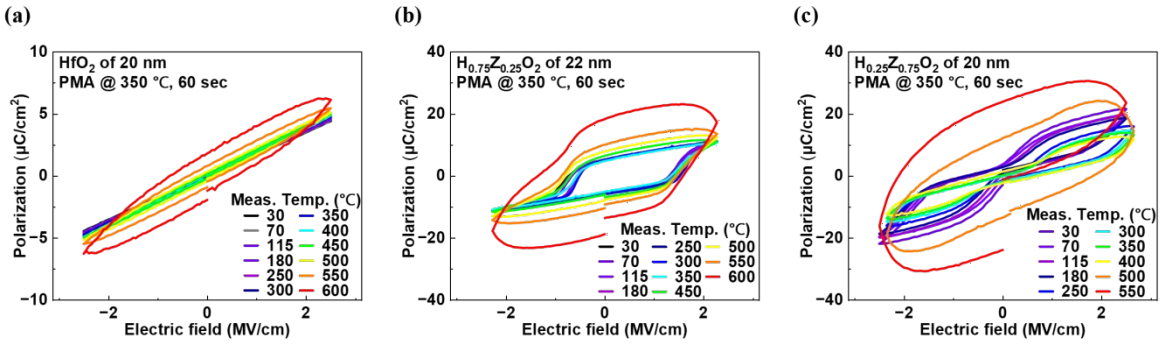

Figure S5. Temperature-dependent experimental results of $H_{1-x}Z_xO_2$ capacitors with film thicknesses greater than 20 nm. P-E hysteresis loops for HZO capacitors with varying Hf:Zr ratios. (a-c) In Hf-rich sample, the transition temperature is very high, whereas in Zr-rich samples, the transition temperature is lower than room temperature, preventing observation of a clear FE-AFE transition.

	HfO_2	$H_{0.75}Z_{0.25}O_2$	$H_{0.5}Z_{0.5}O_2$	$H_{0.25}Z_{0.75}O_2$	ZrO_2
5 nm	-	-	< 30 °C	-	-
7 nm	No FE	> 175 °C	100 °C	< 30 °C	< 30 °C
11 nm			180 °C		
22 nm	No FE	> 600 °C	300 °C	< 30 °C	

Figure S6. Summary of the FE-AFE transition temperature as a function of film thickness and composition in $H_{1-x}Z_xO_2$ capacitors. Pure HfO_2 exhibits no FE behavior, whereas $H_{0.75}Z_{0.25}O_2$ shows

higher transition temperatures compared to $H_{0.5}Z_{0.5}O_2$. In contrast, Zr-rich compositions exhibit FE-AFE transitions below room temperature.

REFERENCES

(1) Zhu, T.; Ma, L.; Deng, S.; Liu, S. Progress in Computational Understanding of Ferroelectric Mechanisms in HfO_2. *npj Comput. Mater.* **2024**, *10*, 188

(2) Mukherjee, B.; Fedorova, N. S.; Íñiguez-González, J. First-Principles Predictions of HfO_2-Based Ferroelectric Superlattices. *npj Comput. Mater.* **2024**, *10*, 153

(3) Oh, S.; Kim, H.; Kashir, A.; Hwang, H. Effect of Dead Layers on the Ferroelectric Property of Ultrathin $HfZrO_x$ Film. *Appl. Phys. Lett.* **2020**, *117* (25), 252906

(4) Kim, T. R.; Saha, A. K.; Gupta, S. K. Analysis of Polarization Switching in HZO/ZrO_2 (HZZ) Nanolaminates Based on Sub-lattice Phase-field Model. *IEEE Proceedings of the 81st Device Research Conference*. **2023**, 1-2

(5) Saha, A. K.; Grisafe, B.; Datta, S.; Gupta, S. K. Microscopic Crystal Phase Inspired Modeling of Zr Concentration Effects in $Hf_{1-x}Zr_xO_2$ Thin Films. *Symp. VLSI Technol.* **2019**, 226-227

(6) Ni, K.; Saha, A.; Chakraborty, W.; Ye, H.; Grisafe, B.; Smith, J.; Rayner, G. B.; Gupta, S.; Datta, S. Equivalent Oxide Thickness (EOT) Scaling with Hafnium Zirconium Oxide High-κ Dielectric Near Morphotropic Phase Boundary. *IEEE Int. Electron Devices Meet.* **2019**, 1-4

(7) Park, M. H.; Kim, H. J.; Lee, Y. H.; Kim, Y. J.; Moon, T.; Kim, K. D.; Hyun, S. D.; Hwang, C. S. Two-Step Polarization Switching Mediated by a Nonpolar Intermediate Phase in $Hf_{0.4}Zr_{0.6}O_2$ Thin Films. *Nanoscale* **2016**, *8* (29), 13898-13907

(8) Kim, K. D.; Lee, Y. H.; Gwon, T.; Kim, Y. J.; Kim, H. J.; Moon, T.; Hyun, S. D.; Park, H. W.; Park, M. H.; Hwang, C. S. Scale-Up and Optimization of HfO_2-ZrO_2 Solid Solution Thin Films for the Electrostatic Supercapacitors. *Nano Energy* **2017**, *39*, 390-399

(9) Shin, J.; Shin, D. H.; Kim, K. D.; Seo, H.; Ye, K. H.; Jeon, J. W.; Kim, T. K.; Paik, H.; Song, H.; Lee, S. H.; Choi, J.-H.; Hwang, C. S. Reversible Modulation of Critical Electric Fields for a Field-Induced Ferroelectric Effect with Field-Cycling in ZrO_2 Thin Films. *J. Mater. Chem. C* **2024**, *12* (38), 15423-15434